A Rheological Study on Kinetics of Poly(butylene terephthalate) Melt Intercalation

Defeng Wu, Chixing Zhou, Hong Zheng

Department of Polymer Science & Engineering, School of Chemistry & Chemical Technology, Shanghai Jiaotong University, Shanghai 200240, People's Republic of China

Received 6 May 2005; accepted 6 July 2005
DOI 10.1002/app.22571
Published online in Wiley InterScience (www.interscience.wiley.com).

ABSTRACT: A multilayered sample with alternatively superposed poly(butylene terephthalate) (PBT) and nonpolar polymer/clay sheets was elaborately prepared to investigate the whole hybridization process of polar polymer. The kinetics of PBT melt intercalation was studied by a rheological approach. The whole intercalation process was demonstrated by the changes of the low-frequencies viscoelastic response with annealing time. The results of the apparent diffusivities and the calculated activation energy indicate that the PBT/clay hybrid formation presents a molecular weight dependence, which may result from the enhancement of interactions between polar groups on PBT chains and the silicate surface. © 2005 Wiley Periodicals, Inc. J Appl Polym Sci 99: 1865–1871, 2006

Key words: intercalation; kinetics; nanocomposites; rheology

INTRODUCTION

In recent years, polymer-layer silicate nanocomposites (PLSN) have attracted great interest from both industry and academia because they frequently exhibit unexpected properties. A large number of polymer–clay nanocomposites have been successfully synthesized through incorporating clay in various polymer matrices such as polyamide,[1–3] polystyrene,[4–6] polypropylene,[7–11] poly(ethylene terephthalate),[12] poly(butylenes terephthalate),[13–16] and so on. PLSN can be prepared by four different methods: solution intercalation, in situ intercalative polymerization, polymer melt intercalation, and exfoliation adsorption. Among them, polymer melt intercalation is the most industrially valuable because of its environmentally benign character, its versatility, and its compatibility with current polymer processing techniques.[4] As a result, the kinetics of the melt intercalation progress, i.e., how polymer chains crawl into the interlayer space of clay forming either an intercalated or an exfoliated nanocomposites, have attracted much attention.

Hitherto many excellent works have been reported on this important question. Vaia et al.[4] first studied the static kinetics of polymer melt intercalation in polystyrene/organoclay. They found that polystyrene melt intercalation in organoclay is controlled by mass transport into the primary particles of the silicate and is not specifically limited by diffusion of the polymer chains within the silicate gallery. The activation energy of hybrid formation is similar to that of the polystyrene self-diffusion in the bulk melt. A further study on the dynamic process of hybrids formation based on nonpolar polymer/organoclay nanocomposites was conducted by Krishnamoorrti et al.[5] and Galgali et al.[9] through a rheological method. But limited by the experimental method, they did not actually explore the intercalating process in the rheometer because the intercalation in their experimental samples produced by extruder had almost completed before the rheological characterization. Li et al.[11] prepared a multilayered sample and succeeded in investigating the intercalation kinetics of the polypropylene/compatilizer/clay hybrids in the rheometer.

However, all these work mainly focus on the intercalation kinetics of the nonpolar polymer/clay or nonpolar polymer/compatilizer/clay hybrids formation, while no report has been found in literature on that of polar polymer/clay hybrids till now. One important reason may be the difficulties to avoid intercalation occurred in the process of samples preparation.

Poly (butylene terephthalate) (PBT) is a typical polar polymer and an engineering plastic with excellent mechanical properties, which has found wide application in fibers and moldings. In our previous work, we studied the rheological behavior of the intercalated PBT/clay nanocomposites and found that the formation of the liquid crystalline-like phase structure in the

Correspondence to: C. Zhou (cxzhou@.sjtu.edu.cn).
Contract grant sponsor: National Natural Science Foundation of China; contract grant numbers: 20174024, 50290090.

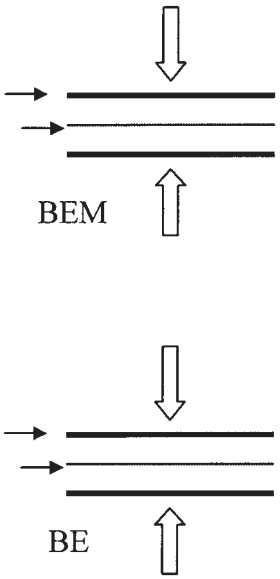

Figure 1 Schematic depicting of the samples preparation.

nanocomposites might be the major drive force for the reorganization of the internal network.[14] Then, to improve the dispersion of clay in the PBT matrix, we used the epoxy resin as a compatilizer preparing the PBT/clay nanocomposites by direct melt compounding. The results from the rheology and properties characterization indicated that the epoxy content influenced the phase morphologies and properties of the nanocomposites remarkably.[15]

In this work, we intend to study on the intercalation kinetics of the PBT/clay hybrids in a rheometer. To investigate the whole intercalation process, we prepared a multilayered sample with alternatively superposed polar PBT and nonpolar polymer matrix/clay sheets to avoid intercalation occurred in the conventional melt blending process, and then, explore the kinetics of hybrids formation by a rheological method.

EXPERIMENTAL

Materials

The poly (butylene terephthalate) (PBT, 1097A, M_n = 23,200; 1097, M_n = 19,200) used in this study was a commercial product of Nantong XinChen Synthetic Material Co. Ltd., P. R. China. Organo-clay (trade name is DK2) with particle size of less than 50 μm was supplied by Zhejiang FengHong Clay Co. Ltd., P. R. China, modified with methyl tallow bis(2-hydroxyethyl) ammonium. The polyethylene (PE) used in this work was a commercial linear-low-density blow molding grade, 'Q400', supplied by Shanghai Petrochemical Co. Ltd., P. R. China. This material has a nominal density of 0.9222 ± 0.0015 g/cm^{-3} and a melt index of 4.0 ± 0.8 (ASTM D 1238).

Sample preparation

PE and DK2 were premixed to fabricate PE/MMT composite, where the loading of DK2 was 8 wt %. Then the PE/MMT composite and PBT were compressed into films with the thickness of ~0.4 mm at 160 and 250°C, respectively. Two PBT and one PE/MMT films were alternatively superposed and compressed into a laminated sheet with the thickness of about 1 mm at 200°C, as seen in Figure 1. Because the process temperature, 200°C, is higher than the melting point of PE but lower than that of PBT, the yielded sheet is composed of two pieces of PBT films adhered together tightly by one piece of PE/MMT films. Hereafter, such a multilayered sample is referred to as BEM sample. A blank sample without clay composed of two PBT and one PE film prepared under the same condition is referred to as BE.

X-ray diffractometry characterization

The degree of swelling and the interlayer distance of the clay in the samples were determined by X-ray diffractometry (XRD) (Fig. 2). The experiments were performed using a Rigaku Dmax-rC diffractometer with a copper target and a rotating anode generator, operated at 40 kV and 100 mA. The scanning rate was 2°/min from 2° to 10°.

Figure 1 shows XRD patterns for DK2, the PE/MMT composite, and the BEM sample annealed for about 4 h in the rheometer at 230°C. The d_{001} peak of the DK2 powder is observed at $2\theta = 3.86°$. Compared with that of the clay powder, the d_{001} peak location of clay in the PE/MMT composite nearly has no movement, while shifts to lower angles (2.42°) obviously in the annealed BEM sample. It elucidates that in the PE/MMT composite, there was no PE chain crawl into the interlayers

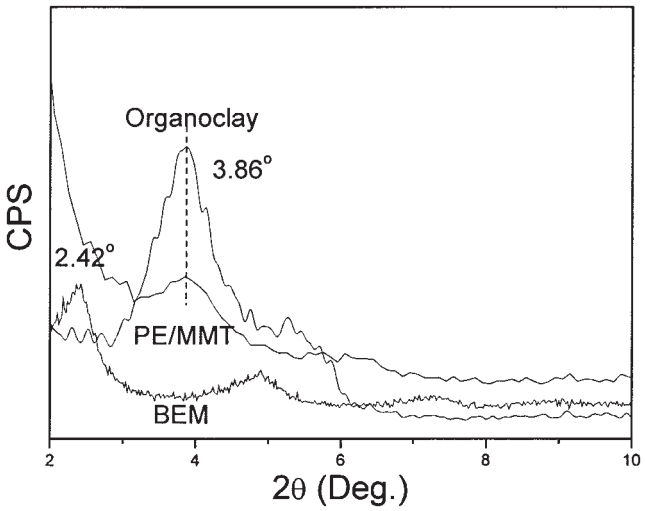

Figure 2 XRD patterns for clay and composites.

of clay. However, for the annealed BEM sample, the d_{001} distance expands to 3.72 nm, which confirms that intercalation happened during annealing.

Morphology characterization

The transmission electron micrographs (TEM) of 80–100 nm thick, ultra-microtomed sections under cryogenic condition were taken using a Hitachi H-860 instrument (Japan) at 100 kV accelerating voltage. The morphologies of the fractured surfaces of the samples were investigated using a Hitachi *S*-2400 scanning electron microscope (SEM) with 15 kV accelerating voltage. The annealed sample was kept in liquid nitrogen for some time and brittle-fractured in liquid nitrogen. An SPI sputter coater was used to coat the fractured surfaces with gold for enhanced conductivity.

Rheological measurements

Rheological measurements were carried out in a small amplitude oscillatory frequency sweep mode (SAOS) on a rheometer (Gemini 200 rheometer, Bohlin Co., UK) equipped with a parallel plate geometry, using 25 mm diameter plates. All measurements were performed with a 200 FRTN1 transducer at a lower resolution limit of 0.02 g cm. The sample was annealed for several hours at a predetermined temperature in the rheometer in a nitrogen environment, and during the annealing period, the frequency sweep was carried out. All the sweeps were conducted at a strain of 1%.

RESULTS AND DISCUSSION

It has been found that the linear viscoelastic response of polymer/silicate hybrids to SAOS is quite different from that of the polymer matrix. For example, compared with that of the polymer matrix, the dynamic modulus G and dynamic viscosity η^* of nanocomposites enhance remarkably at the low frequencies.[9–11,14,15] The change of rheological response such as dynamic moduli and viscosity may be an indicator of the microstructural evolution in nanocomposites. Figures 3(a) and 3(b) present the time evolution of the elastic modulus G' and the loss modulus G'' during annealing at 230°C, respectively. It is clear that the modulus of the sample increases continuously until annealed for about 4 h, indicating that the microstructure of BEM evolves in the annealing period. Both the two modulus become gradually independent of ω at the low frequencies, while G' increases faster than G''. In the process of the microstructural evolution, there are two reasonable molecule movements in the composites system: one is the interdiffusion between two polymer matrices and another is the intercalation of clay particles by polar PBT chains. To find which one is dominant to the enhancement of dynamic modulus, a

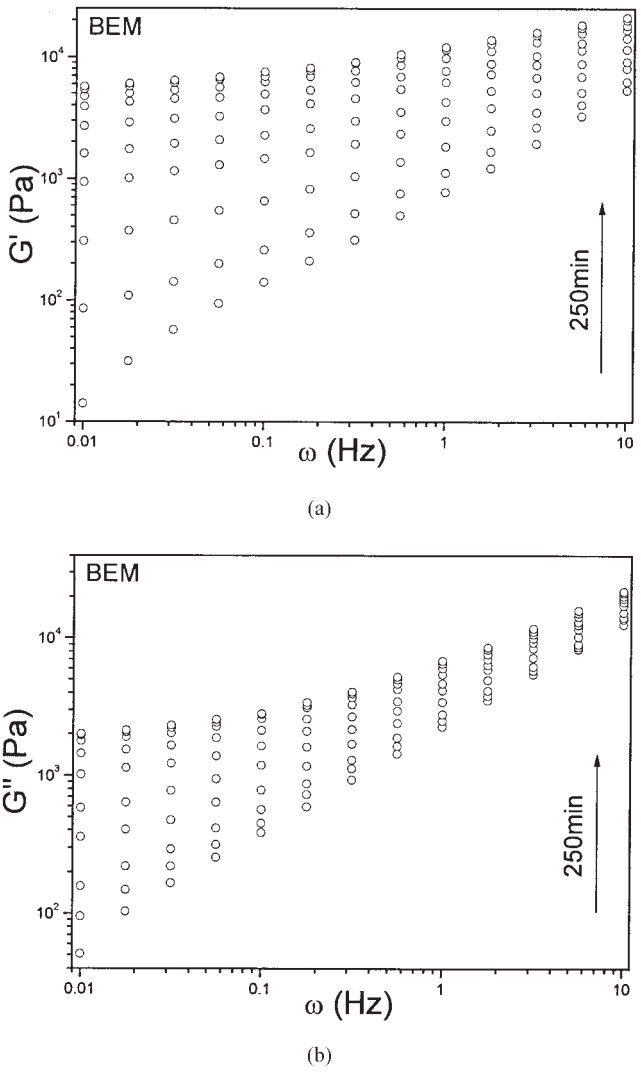

Figure 3 Development of dynamic modulus. (a) storage modulus and (b) loss modulus with annealing time for BEM sample.

multilayered sample of PBT/PE (BE) without clay was prepared under the same processing conditions, and its development of the linear viscoelastic response to SAOS with the annealing time was recorded, as shown in Figure 4. After annealing for about 125 min, although G' of BE presents a monotonically increasing trend, its absolute value at the frequency of 0.01 Hz is only about 10 Pa, while G' of BEM achieves to about 200 Pa under the identical annealing conditions. Therefore, the interdiffusion between PBT and PE chains nearly has no contribution to the enhancement of the lower frequencies modulus.

Moreover, on Figure 5, it can be observed that the moduli curves present a remarkable deviation trend from Cox-Merz rule only after annealing for 25 min, which means that the melt viscoelastic properties of the composites are suffering a transformation from the liquid-like behavior to a solid-like one in the annealing

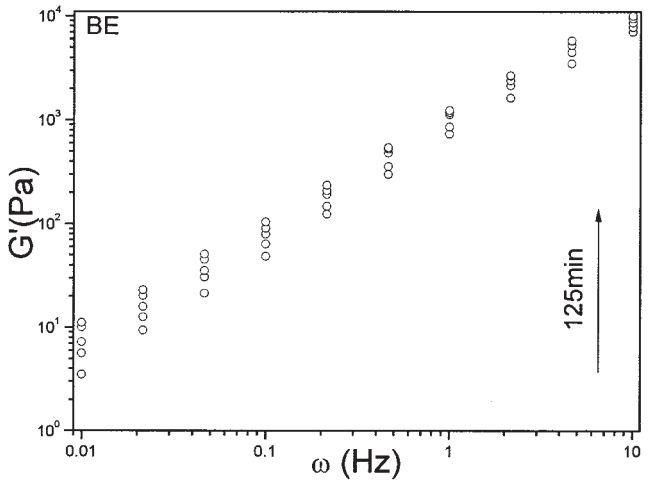

Figure 4 Development of dynamic storage modulus with annealing time for BEM sample.

progress. After annealing for 50 min, the curves exhibit an intersection because of the sharp enhancement of G' at the low frequencies. It is believed that the deviation of the viscoelastic behavior from the linear viscoelastic terminal behavior at low frequencies indicates that PBT chains have intercalated into the silicate interlayer and, as a result, many clay tactoids have detached from primary particles, forming a percolated network due to the physical jamming themselves.[9,10,14]

Figures 6(a) and 6(b) give the SEM photographs of BEM annealed for different times. It can be observed distinctly that there are still many primary particles with the size of 5–20 μm dispersed in the matrix after annealing for about 25 min, while with increase in annealing time, clay particles are hardly found in the matrix, as can be seen in Figure 6(b). During the annealing process, polar PBT chains diffuse near to clay particles at first, and then, the chains penetrate the primary particle from the exterior melts through slits between the tactoids. The penetrated chains then intercalate into interlayer of the tactoids. Those tactoids may disperse more easily into the matrix because of the decrease of the interfacial energy between the matrix and the tactoids. The final morphologies of intercalated tactoids dispersing in the matrix were observed by TEM, as shown in Figure 7.

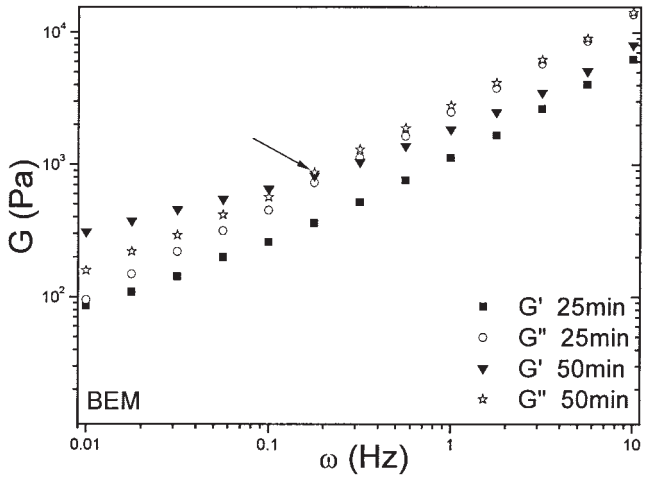

Figure 5 The dynamic moduli for BEM sample.

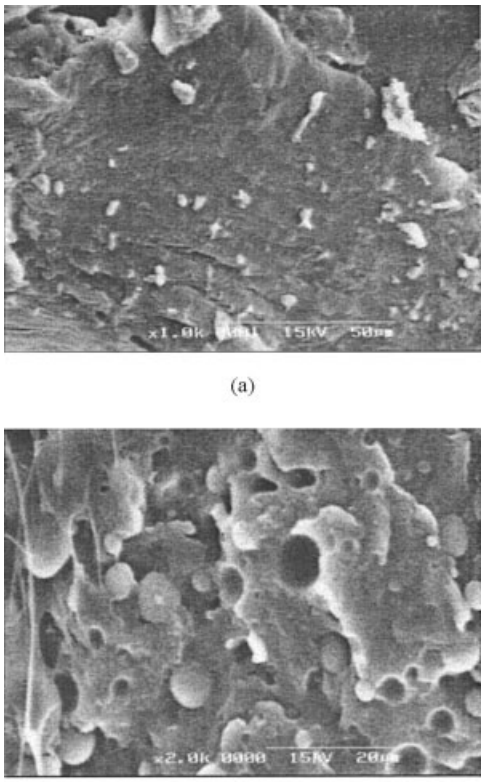

Figure 6 SEM images of BEM sample. (a) after annealing for 20 min at a magnification of 1000 and (b) after annealing for 150 min at a magnification of 2000.

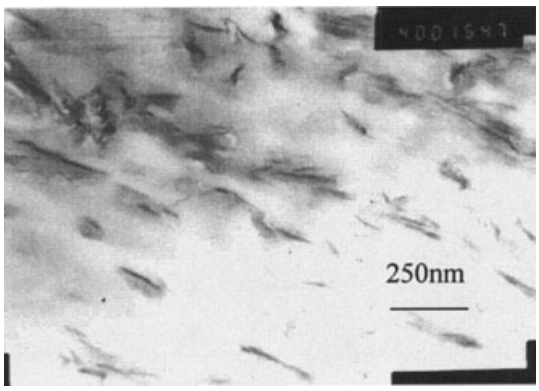

Figure 7 TEM images of BEM sample at a magnification of 40,000.

Figure 6(b) also presents immiscible phase morphologies between PBT and PE matrices. In recent years, there are some researches working on immiscible polymer blend/clay nanocomposites.[17,18] Li and Shimizu[17] studied the PPO/PA-6/clay nanocomposites and found that the dispersed clay platelets played an important role in the control of the PPO/PA6 blend morphology. The selective localization of clay in PA6 phase had significant effects on the morphology of the polymer blend. Mehrabzadeh and Kamal[18] studied the HDPE/PA-66/clay nanocomposites and considered that the clay in the blend nanocomposites played a nucleation agent role and reduces the crystallite size. As a result, it acted as a compatilizer and changed the morphology of the composite system. As for PBT/PE/clay composites in this work, the selective localization of clay in PBT matrix and its effect on the phase morphologies will be discussed in another paper.[19]

The friction of those highly anisotropic platelet-like tactoids tied with PBT chains leads to the formation of percolation network. As a result, the effects of the tactoids on the viscoelastic response are much greater than the primary particles. In percolation system, one of the most important parameters is the critical percolation volume fraction or percolation threshold, ϕ^*. When the volume fraction of filler, ϕ, is above ϕ^*, the three-dimensional filler–filler network structures form. On Figure 3, the enhancement of moduli in the lower frequencies resulted from the increasing tactoids detached from the primary particles with intercalation proceeding. Therefore, it is distinct that the low-frequency modulus have strong dependence on the volume fraction of detached tactoids, $\phi(t)$, the value of which is increasing with annealing time. There is a good approximation for η over the volume fraction range of $0 < \phi(t) < \phi^*$ as follows:[20]

$$\frac{\eta_d(t)}{\eta_m} = \left(1 - \frac{\phi(t)}{\phi^*}\right)^{-2} \quad (1)$$

where η_m and $\eta_d(t)$ is the zero-shear viscosity of the matrix fluid and the zero-shear viscosity of the tactoids dispersing fluid, respectively. Additionally, here the formation of percolation network or physical jamming is indicated by $G' > G''$ in the frequency range of $10^{-2} < \omega < 10^{0}$ Hz.[21] For example, annealed at 230°C, the physical jamming happened at the annealing time of about 50 min. Therefore, the percolation network does not form when the annealing time is shorter, and it is acceptable that the Cox-Merz rule is still valid, and the viscosity measured at $\omega = 0.01$ Hz may be used as the zero-shear viscosity. Using eq. (1), the ratio of $\phi(t)/\phi^*$ can be determined by the data of ϕ(t) before the physical jamming. After the formation of percolation networks or physical jamming, ($\phi(t) \geq \phi^*$), the liquid-like behavior of the composite system transits into the solid-like one, and G' at low frequencies may increase approximately in a power law manner with $\phi(t)$ as follows[22]:

$$G'(t) = G'_{gel}\left(\frac{\phi(t)}{\phi^*}\right)^s \quad (2)$$

where G'_{gel} is the modulus measured at the beginning of percolation formation ($\phi(t) = \phi^*$), the value of s is reported to be near 4.9. Because $G'(t)$ was shown to be weakly dependent on ω at low frequencies after the physical jamming, we suggest $G'(t)$ values measured at $\omega = 0.1$ Hz as the low-frequency plateau G'. Because the accomplishment of intercalation can be indicated by the invariable viscoelastic response to SAOS with annealing time, the ratio of the terminal volume fraction of intercalated tactoids, $\phi(\infty)$ to ϕ^*, was determined by the G' data from the final invariable viscoelastic response by using eq. (2). Therefore, the ratio of $\phi(t)$ to ϕ^*, from the formation of percolation network to the accomplishment of intercalation, can be obtained from the $G'(t)$ data by using eq. (2). Finally, combining the results of $\phi(t)/\phi^*$ before and after physical jamming, the development of the volume fraction ratio, $\phi(t)/\phi^*$, with annealing time in the whole intercalation process can be obtained. Further, dividing $\phi(t)/\phi^*$ by $\phi(\infty)/\phi^*$, the relative volume fraction of the intercalated tactoids, $\phi(t)/\phi^*$, can be determined with no need of the specific value of ϕ^*, which may be considerably obscure for the nanocomposites. Figure 8 gives the resulted value of $\phi(t)/\phi(\infty)$ developing with annealing time.

As mentioned above, the melt intercalation is limited by mass transport of PBT chains into the primary particles, which may be described as a Ficken process with a single, apparent, concentration-independent

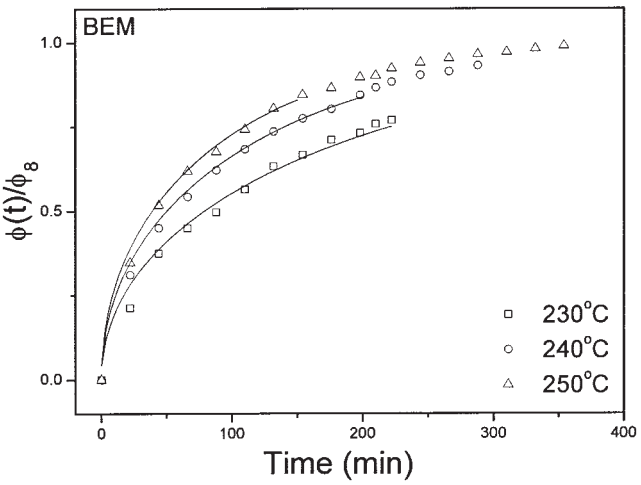

Figure 8 Relative volume fractions of intercalated tactoids as a function of annealing time at 230, 240, and 250°C, respectively. Solid lines are best fits to the data using eq. (3).

diffusivity, D, the ratio of the amount of polymer diffused into primary particles, Q(t), to that at equilibrium, Q(∞) is[4,23]

$$\frac{Q(t)}{Q(\infty)} = 1 - \sum_{m=1}^{\infty} \frac{4}{\alpha_m^2} \exp\left(-\frac{D}{r^2}\alpha_m^2 t \right) \quad (3)$$

where D/r^2 is the effective diffusivity, r is the mean radius of the primary particle, and α_m is the mth positive root of the zeroth-order Bessel function ($J_0(\alpha) = 0$). Considering that the volume fraction of intercalated tactoids, $\phi(t)$, is corresponding to the amount of polymer diffused into primary particles, Q(t), the value of $Q(t)/Q(\infty)$ can be given by the corresponding relative volume fraction of the intercalated tactoids, $\phi(t)/\phi(\infty)$. As seen in Figure 9, the experimental data were fit using eq. (3) to obtain the value of D/r^2 at different annealing temperature. Assuming that r is $\sim$10 μm, the apparent diffusivities, D, can be determined from the effective diffusional rates, and the results are listed in Table I. Furthermore, assuming that the effective diffusivity has an Arrhenius temperature dependence, the activation energy of melt intercalation of PBT chains into clay interlayer, $\Delta E_{\eta 0}$, is $\sim$12.68 $\pm$ 1.2 kJ/mol, which can be obtained by plotting ln D/r^2 *versus* $1/T$, as shown in Figure 9.

The melt intercalation kinetics of a PBT with higher molecular weight (1097A) was also studied via the same rheological method. The activation energy, $\Delta E_{\eta 0}$, is $\sim$15.22 $\pm$ 1.6 kJ/mol. Compared with that of PBT(1097), PBT(1097A) shows a bit larger activation energy in the melt intercalation, suggesting a molecular weight dependence of hybrid formation. Since the contour length of the polymer chains is less than the size of the primary particles or the crystallites, polymer motion within the primary particle is essentially two-dimensional, confined to the silicate galleries or to the small volume between the crystallites. Thus Vaia et al.[4] considered that the 'tube' model, which describes the reptation of polymers in the bulk, might not be used to rationalize the diffusion of polymers in the two-dimensional galleries between the clay layers. Li et al.[11] studied the intercalation kinetics of PP-grafted-MAH with different graft ratio and found that the activation energy of the PP-grafted-MAH with higher graft ratio was larger than that of the PP-grafted-MAH with lower graft ratio. They attributed the enhancement of the activation energy possibly to the increasing interactions of PP-grafted-MAH chains and the surfaces of the silicate layers. Therefore, to PBT(1097A), the one possible reason resulting in the enhancement of the activation energy in contrast to that of PBT(1097) may be the increasing in the polar groups such as hydroxyl, which leads to an enhancement of interactions of PBT chains and the polar silicate surface.

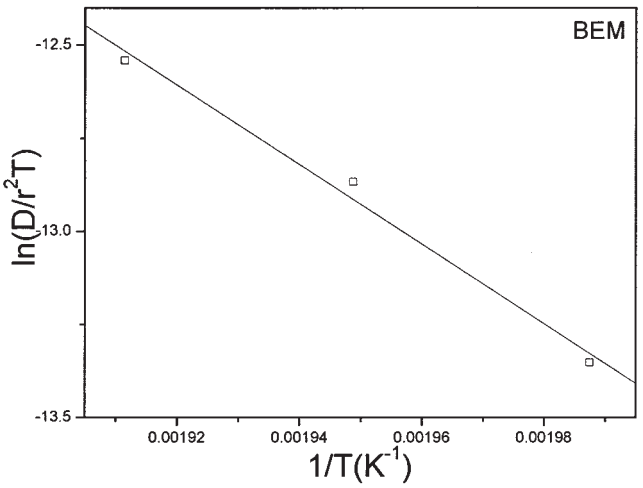

Figure 9 Plot of D/r^2 versus $1/T$.

TABLE I
The Values of the Effective Diffusivity and Apparent Diffusivity at Different Temperatures

	230°C	240°C	250°C
D/r^2 (1/s)	0.0007	0.0013	0.0017
D (cm^2 /s)	0.7×10^{-13}	1.3×10^{-12}	1.7×10^{-12}

CONCLUSIONS

The melt intercalation kinetics of hybrids formation based on polar PBT/clay nanocomposites was studied by a rheological approach. To avoid intercalation, which occurred in the process of samples preparation, an experimental multilayer sample with two PBT and one PE/MMT films were alternatively superposed and compressed into a laminated sheet. The whole development of the relative volume fraction of intercalated tactoids can be obtained from the rheological parameters of viscosity and storage modulus in lower frequencies, which could be used to determine the apparent diffusivities for mass transport into the primary particles at the different temperatures. The results of the calculated activation energy indicate that the PBT/clay hybrid formation presents molecular weight dependence, which may result from the enhancement of interactions of polar groups on PBT chains and the silicate surface.

References

1. Kojima, Y.; Usuki, A.; Kawasumi, M.; Okada, A.; Kurauchi, T.; Kamigaito, O. J Polym Sci Part A Polym Chem 1993, 31, 983.
2. Wu, Z. G.; Zhou, C. X.; Qi, R. R.; Zhang, H. B. J Appl Polym Sci 2002, 83, 2403.
3. Wu, Z. G.; Zhou, C. X. Polym Test 2002, 21, 479.

4. Vaia, R. A.; Janndt, D. K.; Kramer, E. J. Macromolecules 1995, 28, 8080.
5. Krishnamoorrti, R.; Vaia, R. A.; Giannelis, E. P. Chem Mater 1996, 8, 1728.
6. Manias, E.; Chen, H.; Krishnamoorrti, R.; Genzer, J.; Kramer, E. J.; Giannelis, E. P. Macromolecules 2000, 33, 7955.
7. Kawasumi, M.; Hasegawa, N.; Kato, M.; Usuki, A.; Okada, A. Macromolecules 1997, 30, 6333.
8. Usuki, A.; Kato, M.; Okada, A.; Kurauchi, T. J. J Appl Polym Sci 1997, 63, 137.
9. Galgali, G.; Ramesh, C.; Lele, A. Macromolecules 2001, 34, 852.
10. Li, J.; Zhou, C. X.; Wang, G. J Appl Polym Sci 2003, 89, 3609.
11. Li, J.; Zhou, C. X.; Wang, G.; Zhao, D. J Appl Polym Sci 2003, 89, 318.
12. Ke, Y.C.; Long, C.F.; Qi, Z. N. J Appl Polym Sci 1999, 71, 1139.
13. Li, X. C.; Kang, T.; Cho, W. J.; Lee, J. K.; Ha, C. S. Macromol Rapid Commun 2001, 21, 1040.
14. Wu, D. F.; Zhou, C. X.; Xie, F.; Mao, D. L.; Zhang, B. Eur Polym J 2005, 41, 2199.
15. Wu, D. F.; Zhou, C. X.; Zheng, H.; Mao, D. L.; Zhang, B. Polym Degrad Stab 2005, 87, 511.
16. Wu, D. F.; Zhou, C. X.; Xie, F.; Mao, D. L.; Zhang, B. Polym Polym Compos 2005, 13, 61.
17. Li, Y. J.; Shimizu, H. Polymer 2004, 45, 7381.
18. Mehrabzadeh, M.; Kamal, M. R. Polym Eng Sci 2004, 44, 1152.
19. Wu, D. F.; Zhou, C. X.; Zhang, M. J Appl Polym Sci, submitted.
20. Bicerano, J.; Douglas, K. F.; Brune, D. A. J Polym Sci Part C Rev Macromol Chem Phys 1999, 39, 561.
21. Yanez, J. A.; Laarz, E.; Bergstrom, L. J Colloid Interface Sci 1999, 209, 162.
22. Rueb, C. J.; Zukoski, C. F. J Rheol 1997, 41, 212.
23. Gell, C. B.; Graessley, W. W.; Fetters, L. J. J Polym Sci Part B: Polym Phys 1997, 35, 1933.